Journal of Microencapsulation, June 2008; 25(4): 267–274

Alginate bead fabrication and encapsulation of living cells under centrifugally induced artificial gravity conditions

STEFAN HAEBERLE[1], LARS NAEGELE[2], ROBERT BURGER[1], FELIX VON STETTEN[1,3], ROLAND ZENGERLE[1,3], & JENS DUCRÉE[1,3]

[1]*HSG-IMIT–Institute for Micromachining and Information Technology, Villingen-Schwenningen, Germany,* [2]*Laboratory for Process Technology, and* [3]*Department of MEMs Applications, Department of Microsystems Engineering (IMTEK), University of Freiburg, Freiburg, Germany*

(Received 10 July 2007; accepted 31 January 2008)

Abstract
This study presents a novel method for the direct, centrifugally induced fabrication of small, Ca^{2+}-hardened alginate beads at polymer-tube micronozzles. The bead diameter can arbitrarily be adjusted between 180–800 μm by the nozzle geometry and spinning frequencies between 5–28 Hz. The size distribution of the main peak features a CV of 7–16%, only. Up to 600 beads per second and channel are issued from the micronozzle through an air gap towards the curing agent contained in a standard lab tube ('Eppi'). Several tubes can be mounted on a 'flying bucket' rotor where they align horizontally under rotation and return to a vertical position as soon as the rotor is at rest. The centrifugally induced, ultra-high artificial gravity conditions (up to 180 *g*) even allow the micro-encapsulation of alginate solutions displaying viscosities up to 50 Pa s, i.e. ~50 000 times the viscosity of water! With this low cost technology for microencapsulation, HN25 and PC12 cells have successfully been encapsulated while maintaining vitality.

Keywords: *Centrifugal, micronozzle, droplet formation, alginate bead, cell encapsulation*

Introduction

Microencapsulation concerns the coating of a solid or liquid phase with a layer providing a certain level of protection. The properties of the layer can often be tuned by physico-chemical means. There are three major fields of application for microencapsulation.

The first field is food production, e.g. the enhancement of nutrition by encapsulated vitamins, minerals or even pro-biotic bacteria (Sultana et al. 2000, Kailasapathy 2002). Also in the cosmetic industry, encapsulation of colours and flavours became more and more popular within the last years, sometimes only for optical and no functional reasons. However, both fields of application require quite large (100–1000 μm) microcapsules while monodispersity (narrow size distribution) is of minor concern. That is why mostly conventional encapsulation technologies like spray drying are sufficient to meet the requirements.

The third rapidly growing field of application is drug delivery. This field can be categorized into the encapsulation and controlled release of pharmaceuticals, e.g. for cancer therapy (Gibbs et al. 1999) and the encapsulation of living cells to replace failed body functions, e.g. in diabetes. For these applications, small capsule sizes and monodisperse size distributions are key for the diffusively governed mass transport.

This paper focuses on the encapsulation of living cells into biocompatible polymers for *in-vivo* applications. For these applications, the biopolymer alginate is the most commonly used material (Sugiura et al. 2005), possessing a proven record in long-term biocompatibility tests (De et al. 2003). Alginate is produced from brown algae and is called Na-alginate in the liquid state. As soon as Na-alginate gets in contact to a solution containing Ca^{2+} ions, it swiftly hardens to the Ca-alginate (sol-gel transition).

Correspondence: Stefan Haeberle, HSG-IMIT–Institute for Micromachining and Information Technology, Wilhelm-Schickard-Straße 10, 78052 Villingen-Schwenningen, Germany. Tel: +49 761 203 7476. Fax: +49 761 203 7539. E-mail: stefan.haeberle@hsg-imit.de

ISSN 0265–2048 print/ISSN 1464–5246 online © 2008 Informa UK Ltd.
DOI: 10.1080/02652040801954333

The semi-permeable Ca-alginate coating protects the encapsulated alien cells from the immune system while still permitting the diffusive transport of nutrition and metabolites to keep the cells alive (Orive et al. 2003). To guarantee a sufficient diffusive mass transport, the diameter of the microcapsules should not exceed 300 μm (Renken and Hunkeler 1998). However, handling problems, in particular during implantation, set a lower size limit. Overall, an optimum size range for cell therapy of 50–300 μm has been postulated (Sugiura et al. 2005). The encapsulation of insulin-producing pancreas cells into alginate beads was pioneered in 1980 (Lim and Sun 1980). The microbeads were implanted into laboratory rats, showing an elongated period of blood glucose regulation (> 20 days) compared to non-encapsulated islets (~10 days).

Two major technical challenges have to be mastered for the production of alginate beads. First, the surface tension and the viscous forces which counteract the droplet break-off at the nozzle have to be overcome. Secondly, the curing of the alginate beads has to take place while ruling out clogging and agglomeration. In the literature, there are two main approaches for encapsulation.

Direct methods are based on the dispensing of Na-alginate droplets through an air gap straight into a $CaCl_2$ solution where they instantaneously harden. The air gap prevents premature hardening and thus clogging of the nozzle. Established technologies are based on pressure-driven flows through sub-millimetre sized nozzles. The droplet break-off is supported by a vibration of the nozzle (BRACE 2006), an additional cutting-blade (Prusse et al. 1998) or air-flow (Sugiura et al. 2007). However, all these conventional techniques require a rather complex and costly apparatus, whereas a wider acceptance of cell-encapsulation based therapies requires the availability of affordable and reliable in-house fabrication methods.

Indirect methods rely on the formation of Na-alginate droplets in a second immiscible liquid phase like oil using (microfluidic) emulsification methods (Sugiura et al. 2005, Liu et al. 2006). The hardening of the droplets is, for instance, initiated by a change in the pH of the continuous phase to form Ca-alginate beads within several seconds to minutes (Tan and Takeuchi 2006). Due to the additional washing procedure required to remove residual oil from the bead surface, the throughput of these indirect methods thus tends to be much smaller compared to direct methods.

This paper presents centrifugally induced microencapsulation (Haeberle et al. 2007a). The novel technique can process highly viscous biopolymer solutions (up to 50 000 times the viscosity of water) while being sufficiently gentle to maintain the vitality of the cells. This is not possible with presently available encapsulation technologies (Koch et al. 2003). In this scheme, a commercially available polymer micro-nozzle (Streule et al. 2004) is spun on a centrifuge to dispense alginate droplets through an air gap into a standard *Eppendorf* tube ('*Eppi*') mounted on the flying bucket rotor. The tube contains an aqueous $CaCl_2$ solution to perform diffusion based hardening to Ca-alginate beads.

The first section outlines the functional principle of quasi-static droplet generation and its adoption on the centrifugal microfluidic platform. The next section describes the experimental results for the alginate bead formation, their size distribution and size control. Within the last section, the encapsulation of living cells under the impact of the centrifugally induced artificial gravity is presented.

Principle of operation

Droplet generation under terrestrial and centrifugal conditions

The two fundamental droplet formation mechanisms at a nozzle of inner diameter d_n exposed to gravity are depicted in Figure 1. The quasi-static droplet formation is referred to as 'dripping', where a droplet breaks off once the gravity-induced pulling force $F_g = m_{drop} g$ exceeds the surface-tension induced counter force $F_\sigma = \pi d_n \sigma_{drop}$ (Figure 1(a)). At elevated flow rates, the inertia of the liquid tends to issue elongated jets from the nozzle (Figure 1(b)). Due to the Rayleigh instability, the jet subsequently tends to disintegrate. This 'airborne' break-off is of statistical nature (Utada et al. 2005) and thus compromises the objective of the narrow droplet size distribution. This work therefore focuses on the quasi-static, flow-rate restricted dripping regime.

By equating the counteracting forces F_g and F_σ, one obtains a droplet diameter

$$d_{drop} = \sqrt[3]{\frac{6\, d_n\, \sigma_{drop}}{\rho_{drop}\, g}} \qquad (1)$$

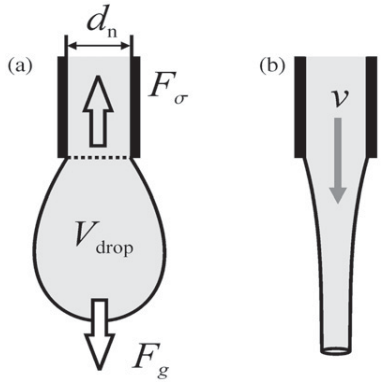

Figure 1. (a) Dripping out of a micronozzle under the impact of the gravitational force F_g pulling out the liquid against the counteracting surface tension force F_σ. (b) At elevated flow rates v, a jet is issued from the nozzle, which later tends to disintegrate in a statistical fashion (Rayleigh instability).

with the density ρ_{drop} and the surface tension σ_{drop} of the liquid. In this experimental setup, a commercially available nozzle (tube) was chosen with an inner diameter $d_n = 127\,\mu m$ (Streule et al. 2004). Under terrestrial conditions ($g = 9.81\,ms^{-2}$), equation (1) yields a large droplet size d_{drop} of 1.7 mm for a 2-w% Na-alginate solution (ρ_{drop} and σ_{drop} as specified in Table I).

Due to the weak scaling $d_{drop} \sim d_n^{1/3}$, the nozzle diameter d_n would have to be reduced into the submicron range in order to shift d_{drop} to the targeted droplet diameters of a few hundred micrometres. On the one hand, this puts severe challenges on the fabrication of the nozzle. On the other hand, the droplet generation frequency would be way too low for an industrial production in a merely gravity driven flow. By applying an additional pumping pressure, the throughput could be raised, which pushes the break-off dynamics into the undesired jetting regime in return. Most seriously, however, the cells would not fit through the sub-micron micronozzle anymore, thus ruling out a successful encapsulation.

To generate small droplets without choking the droplet rate, one therefore shrank the droplet diameter d_{drop} by imposing centrifugally induced artificial gravity conditions

$$g_{art} = \omega^2 r \qquad (2)$$

Table I. Main measured material parameters of the alginate solutions for microbead fabrication.

Material	Mass density ($g\,cm^{-3}$)	Surface tension ($m\,Nm^{-1}$)	Viscosity ($Pa\,s$)**
2 w-% Na-alginate	0.997	65.45*	2.75
4 w-% Na-alginate	1.006	–	17.47
5 w-% Na-alginate	1.018	–	36.42
6 w-% Na-alginate	1.017	–	49.78

*Pending drop method: mean value ($n = 4$); **dynamic viscosity at $20\,s^{-1}$ shear rate.

with the radial position of the nozzle r and the angular frequency ω. For the nozzle tip positioned at a radius $r = 5.7\,cm$ and a typical experimental spinning frequency $\omega = 176\,rad\,s^{-1}$ (28 Hz), the artificial gravity calculates to $g_{art} \approx 1766\,m\,s^{-2}$, i.e. a 180-fold increase with respect to terrestrial gravity! To still stay within the dripping regime at high centrifugal 'pulling' forces, the flow rate is throttled by a sufficient length of the narrow nozzle tube. Inserting equation (2) into equation (1), this centrifugal dripping process thus delivers a droplet diameter d_{drop} of 305 μm for a 2 w-% Na-alginate solution.

Setup for centrifugal droplet generation

In this novel, rotor based setup, droplets were generated within the dripping regime at the micronozzle tip of a commercially available standard polymer tube (Figure 2). The inner end of the tube is connected to a 500 μL reservoir containing the Na-alginate solution. The receiving standard Eppendorf tube ('Eppi') with a volume capacity of 1.5 mL or 2-mL contains the $CaCl_2$ solution. The Eppi is held in a flying bucket holder which is free to align according to the frequency-dependent centrifugal field (f_ω). Therefore, the dispensed alginate droplet impacts perpendicular to the air–liquid meniscus within the tube. Upon halting the rotor, gravity prevails to realign the tube in a vertical position. The Eppendorf tube can be taken out of the rotor for further processing, e.g. culturing or analysis. Due to the intrinsic rotational symmetry, several nozzles can be operated simultaneously in a spoke-like alignment on the same rotor.

Hardening

The sol-gel transition of the alginate beads initiates at the interface between droplet and $CaCl_2$ solution (100 mM) and continues inbound until the entire droplet forms a solid microbead. While the hardening of the outer shell occurs quite rapidly upon contact with the curing agent, the Ca^{2+} ions have to diffuse through an

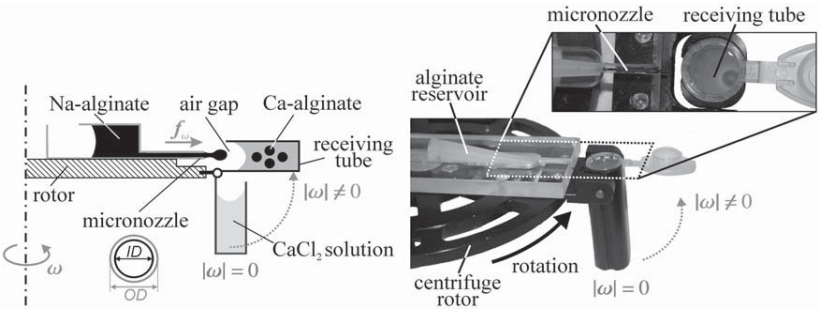

Figure 2. (Left) Functional principle of the rotating micronozzle set-up. At a frequency of rotation $\omega > 0$, an alginate solution is dispensed from a micronozzle and 'falls' under the impact of the artificial gravity (f_ω) into a receiving tube held in a flying bucket arrangement and containing the $CaCl_2$ hardening agent. (Right) Photo of the experimental centrifugal set-up for Ca-alginate bead fabrication.

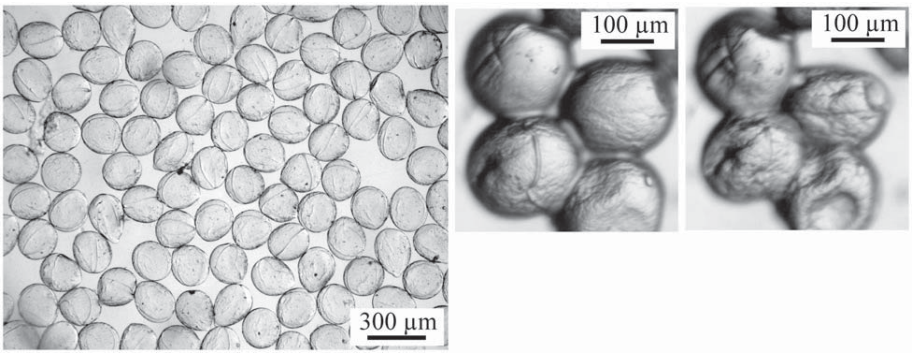

Figure 3. Left: microscopic picture of Ca-alginate beads fabricated using the 127 µm/165 µm micronozzle at a frequency of 28 Hz. Right: Beads exhibit a surface topology after drying in air which is possibly associated with the liquid bridge observed during the droplet break-off in Figure 4(f).

increasingly thick layer of hardened alginate at the later stages.

Due to the rapid hardening of the outer shell, a direct contact between the alginate and the $CaCl_2$ solution at the issuing micronozzle would lead to fatal clogging. One possible solution to avoid clogging is the dispersion of alginate into an intermediate, immiscible oil-phase (Tan and Takeuchi 2006). However, this method is much slower and requires an additional washing of the beads.

A more simple approach for the hardening of alginate beads is presented here. This study interspersed an air gap as a spacer between the alginate solution issued from the nozzle and the $CaCl_2$ solution stored in a receiving tube (Haeberle et al. 2007a). Using an air spacing instead of a liquid also obviates the need of subsequent washing steps for the retrieval of the beads. A surfactant (0.1 w-% Tween-20) supports the swift penetration of the alginate droplet into the liquid bulk to suppress the agglomeration with previously dispensed droplets settling at the liquid meniscus or the bursting of the droplets at high impact velocities.

Na-alginate solution

The main material parameters of the utilized Na-alginate solutions (*Roth*, order number: 9180.1) for different concentrations are compiled in Table I. Na-alginate is a non-*Newtonian* (thixotropic) liquid exhibiting a non-linearly decreasing dynamic viscosity towards elevated shear rate. The highest, 6 w-% concentration used in these experiments exhibits a viscosity of 49.78 Pa s, corresponding to ~50 000 times (!) the viscosity of water.

The processing of Na-alginate solutions at concentrations beyond 2 w-% is hard to realize using conventional techniques (Koch et al. 2003) and thus constitutes a strong selling point of the centrifugal microencapsulation technology. This is important because the mechanical stability of the Ca-alginate beads increases with the alginate concentration (Martinsen et al. 1989) and an improved stability is advantageous during implantation (Peirone et al. 1998).

Experimental results

Droplet formation under rotation

Figure 3 displays Ca-alginate micro-beads that were fabricated using the 127 µm/165 µm nozzle (inner and outer diameter, ID/OD) immersed in an aqueous environment. Along the drying process in air, the beads continuously shrink (Figure 3, right). A fraction of the beads apparently features a surface topology which is likely to result from the liquid-bridge that has been observed during the droplet break-off (Figure 4(f)).

Size distribution

The diameter of the micro-beads (2 w-% Na-alginate) fabricated using the 127 µm/165 µm nozzle at different frequencies of rotation (17–28 Hz) is displayed in Figure 5 (left). The size distribution of a few thousand beads has been measured using a laser diffractometer (*Beckman Coulter*, LS230). The generation of beads is suppressed at frequencies below 17 Hz where the surface tension force still over-rules the centrifugal field. Proceeding beyond this lower threshold frequency into the working range of the micronozzle, the average size of the micro-beads decreases due to the inverse scaling $d_{\mathrm{drop}} \sim {g_{\mathrm{art}}}^{-1/3} \sim \omega^{-2/3}$ with the frequency of rotation ω (2). The main peak displays a narrow width (CV between 7–16%) which is attributed to the pulse-free centrifugal droplet generation mechanism.

A rate of 600 beads per second has been recorded for the 127 µm/165 µm micronozzle at 28 Hz, corresponding to a discharge of $\sim 1.9\,\mu\mathrm{L\,s^{-1}}$ per nozzle. The droplet rate depends on the length and the diameter of the micronozzle as well as the viscosity of the dispensed solution. In the working range, the rate also rises with the frequency ω.

However, with an increasing droplet generation rate, the time interval between two subsequent droplets impacting at the air–liquid interface diminishes. Above frequencies of 22.5 Hz, this eventually leads to merged droplets, appearing as multiples of the initial diameter in the upper end of the size distribution.

The mean bead diameters (d_{50}) measured for both micronozzles (127 µm/165 µm and 511 µm/562 µm) over the frequency of rotation ω are shown in Figure 5 (right). The coalescence of droplets sets a practical upper limit for the frequency of rotation, amounting to 14 Hz and 28 Hz for the 511 µm/562 µm and 127 µm/165 µm nozzles, respectively.

Besides the experimentally measured bead size, the theoretically calculated droplet diameters of the Na-alginate droplets corresponding to equations (1) and (2) are plotted in the graph (dashed line) in Figure 5 (right). Evidently, the theoretical diameters of the Ca-alginate beads are systematically located above the experimentally observed values. This systematic deviation can be explained, to a certain extent, by a reduction of the diameter of 32% associated with the gelification process (Wolters et al. 1992), as indicated by the solid line (theoretical Ca-bead diameter after gelification and the accompanying shrinkage).

The good qualitative agreement between the experimental and the theoretical data corroborates the validity of the applied dripping theory. The measured bead diameter (Figure 5, right) also demonstrates the capability to fabricate Ca-alginate microbeads with diameters between 180–800 µm using a suitable micronozzle geometry and tuning the droplet formation by changing the frequency of rotation.

High-concentration alginate microbeads

Ca-alginate beads made from 4, 5 and 6 w-% Na-alginate solution and using the 511 µm/562 µm nozzle at a frequency of 40 Hz are depicted in Figure 6. The beads show an increasing tail towards growing Na-alginate concentrations which apparently emerges from the hardening of the bridge that establishes during the droplet formation at the micronozzle (Figure 4(f)).

For the highest concentration (6 w-%), the tail imposes an elongated, non-spherical shape of the Ca-beads as the highly viscous droplet cannot relax to assume a spherical shape within the short transfer time between the micronozzle and the receiving tube. However, complying with equation (1) derived for the quasi-static dripping regime, the size of the Ca-alginate beads does not change significantly with increasing viscosity (concentration).

Figure 6 demonstrates the general capability of the centrifugal encapsulation technology to handle highly

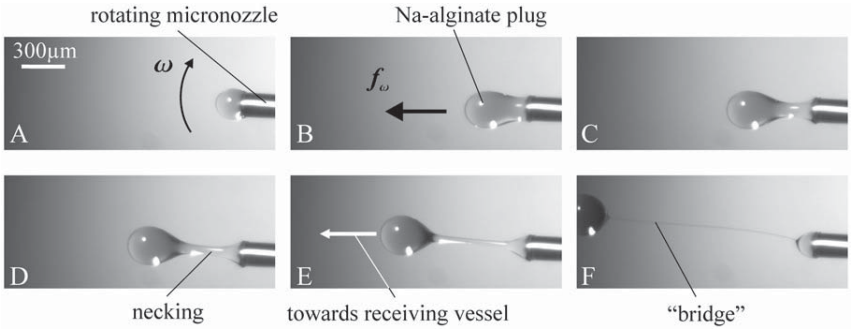

Figure 4. Stroboscopic sequence visualizing the droplet break-off under rotation at the 127 µm/165 µm micronozzle at 22.5 Hz (Grumann et al. 2005). Frame F shows a liquid 'bridge' between the issued droplet and the nozzle.

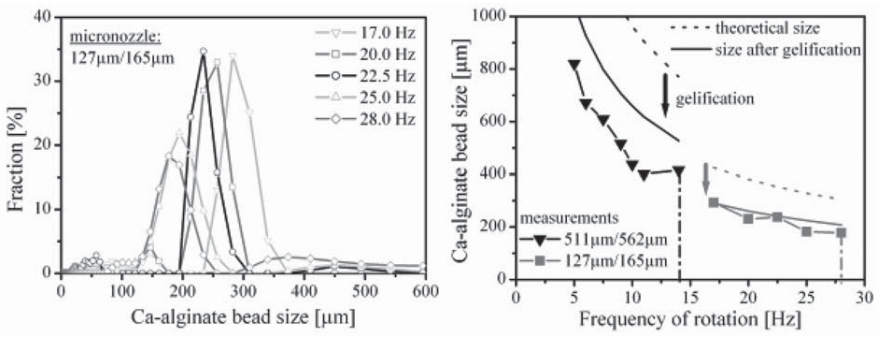

Figure 5. Left: Size distribution of the beads, fabricated using the 127 µm/165 µm nozzle. Right: Mean diameter (d_{50}) of the microbeads over the frequency of rotation. The size shrinks towards elevated frequencies due to the prevalence of the artificial gravity field according to equations (1) and (2).

viscous liquids. This is of great importance for the encapsulation of cells as the mechanical stability of the Ca-beads increases with the Na-alginate concentration (Martinsen et al. 1989). A high stability is, in turn, favourable for the implantation of encapsulated cells (Peirone et al. 1998).

The droplet formation rate is slowed down for higher viscous solutions. In particular for small frequencies of rotation and small micronozzle dimensions, the droplet formation process can even extend over several seconds! In order to set a certain production rate, the frequency of rotation can, of course, be elevated.

Encapsulation of cells

The incorporation of cells into homogeneous alginate-capsules (Peirone et al. 1998, Sugiura et al. 2005, Tan and Takeuchi 2006) represents the first step for further encapsulation into a liquid core capsule, for instance according to the alginate/poly-L-lysine (PLL)/alginate technology (Renken and Hunkeler 1998, Joki et al. 2001, Koch et al. 2003). The goal of this work is to prove the successful encapsulation of cells into Ca-alginate beads while maintaining their vitality using the centrifugal encapsulation technology.

Centrifugal cell-encapsulation

For the encapsulation studies, two cell types were used: HN25 and PC12 cells. Both were cultured following standard procedures. The Na-alginate solution was prepared using D-PBS buffer (without $CaCl_2$ and $MgCl_2$) instead of water in order to comply with the osmotic pressure of the cells and to avoid an unwanted hardening of the alginate. As receiving liquid, the same 100 mM $CaCl_2$-solution—without an additional surfactant—was used as in the prior experiments. Prior to the encapsulation process, the solutions (Na-alginate and $CaCl_2$) as well as the micronozzle and the tubes were

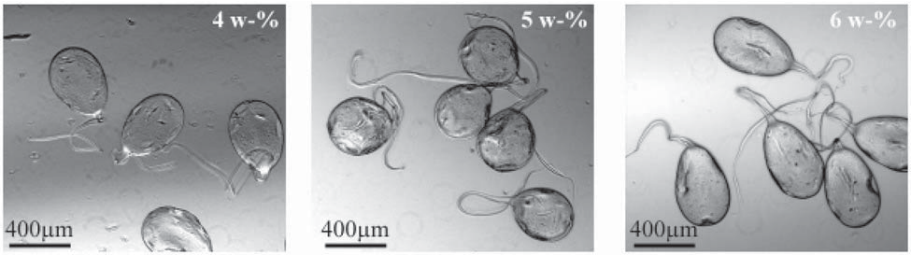

Figure 6. Micro-beads made from high-concentrated (4, 5 and 6 w-%) Na-alginate solution using the 511 µm/562 µm micronozzle (frequency of rotation: 40 Hz).

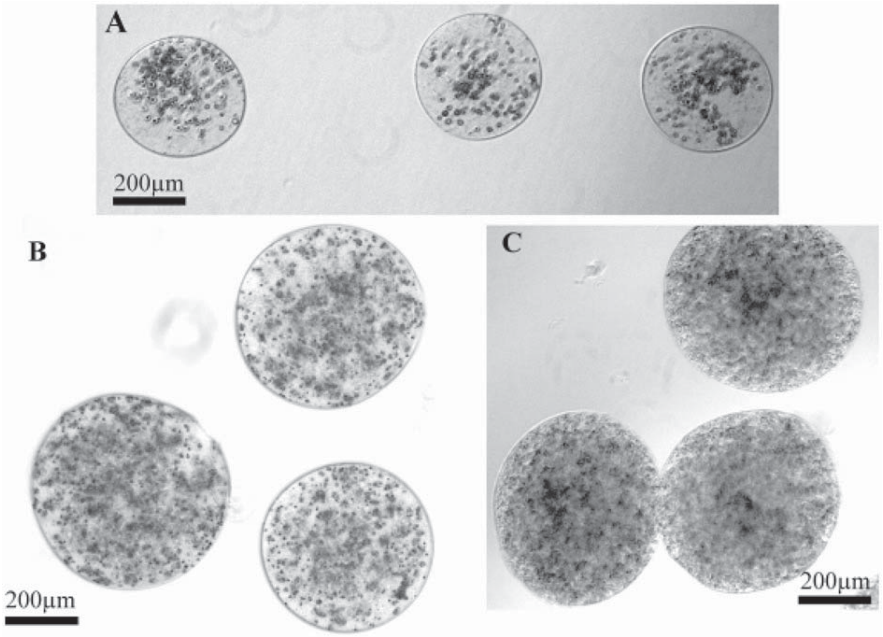

Figure 7. (a) HN25 cells (2 w-% alginate, 127 µm/165 µm nozzle, 20 Hz). (b) Low concentration of PC12 cells (2 w-% alginate, 511 µm/565 µm nozzle, 20 Hz). (c) High concentration of PC12 cells (2 w-% alginate, 511 µm/565 µm nozzle, 20 Hz).

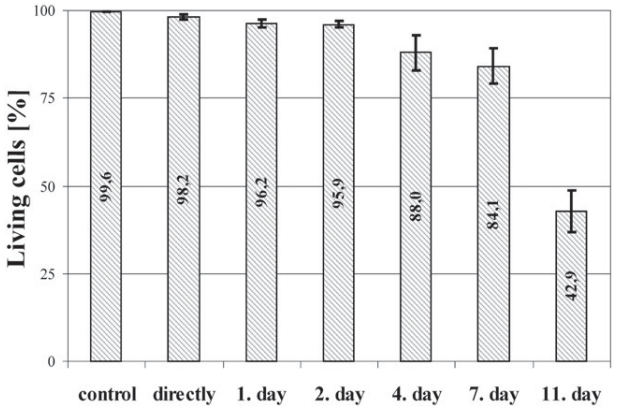

Figure 8. Vitality of the cells (PC12) before and directly after the encapsulation (2 w-%). Almost no losses linked to the encapsulation process are observed. After several days of culturing, the amount of living cell decreases down to 42.9% at day 11.

sterilized in an autoclave (15 min @ 121°C for liquids and 20 min @ 121°C for solids).

The cells are released from the floor of the culturing flask and re-suspended in a 50 µL culture medium. The cell suspension is mixed with 500 µL of the Na-alginate solution and placed into the micronozzle reservoir which is mounted on the rotor (Figure 2). Afterwards, a batch of the cell-alginate suspension is encapsulated by spinning for 5 min at 20 Hz. The cell-containing Ca-alginate beads within the receiving tube are then extracted from the $CaCl_2$, re-suspended in 5 mL culture medium and placed in a Petri-dish for optical investigation or vitality testing.

Figure 7 shows ensembles of HN25 and PC12 cells encapsulated into Ca-alginate beads (2 w-%) using different micronozzles and cell concentration. The high concentration PC12 beads have been used for the long-term vitality tests as described in the following.

Cell vitality

The number of living cells has been measured before the encapsulation process by colouring the cells with trypan blue and counting them in a *Neubauer* counting chamber. The encapsulated cells are released by incubating the Ca-alginate beads into a 0.1 M trisodium citrate solution for 5 min (Lee et al. 1991). Afterwards, they are re-suspended in culture medium for the vitality test. The results for the high PC12 concentration experiments are reproduced in Figure 8, displaying a slight decrease of the number of living cells directly after the encapsulation compared to the control test (from 99.6% to 98.2%). Also, after 2 days of encapsulation, the majority of the cells are still alive (95.9%) and a significant decrease of vitality is not observed until the fourth day (88% down to 42.9% at day 11). The released cells have been further cultivated in *Petri*-dishes, showing a similar vitality in terms of adherent confluent growth compared to the control lines.

Conclusion

This study added micro-bead fabrication capabilities to the recently introduced centrifugal multiphase microfluidic platform (Haeberle et al. 2007a, b). By adjusting the spinning frequency and the nozzle geometry, the main peak of the alginate solution can be pushed below 200 µm, exhibiting a CV down to 7% only. This size of the alginate microbeads is compatible with applications for therapeutic cell encapsulation. Compared to existing methods, this novel centrifugal scheme offers pulse-free und thus well reproducible droplet generation.

The ability of the centrifugal encapsulation technology to even process highly viscous liquids within small-diameter and thus high-resistance micronozzles under the impact of the centrifugally induced artificial gravity conditions has been shown for highly concentrated Na-alginate solutions (viscosity enhanced up to a factor of 50 000 with respect to water). Finally, two different cell types (PC12 and HN25) are successfully encapsulated into single Ca-alginate beads. The gentle, centrifugally induced droplet break-off allows one to conserve the vitality of the cells.

Besides the capability to process high-viscous liquids, another advantage of the centrifugal microencapsulation technology is its conceptually simple and low-cost set-up. The complete encapsulation equipment could be realized in an enclosed disposable polymer tube similar to spin-columns. These sterilized containers can be processed in any standard flying-bucket rotor at a high degree of parallelization. No additional equipment other than the disposable is required, thus obviating many cleaning and sterilization steps which are common in present technologies. The here presented technology hence enables even a resource-poor research lab to carry out encapsulation experiments on demand and to push the encapsulation of living cells technology for drug delivery in general.

Acknowledgements

We would like to thank Sascha Lutz and Stefanie Reinbold for supporting the cell encapsulation experiments as well as Wolfgang Streule and Lutz Riegger for providing the polymer micronozzles.

References

BRACE GmbH. 2008. Company homepage. Available online at: www.brace.de, accessed 2008.

de Vos P, van Hoogmoed CG, van Zanten J, Netter S, Strubbe JH, Bussacher HJ. 2003. Long-term biocompatibility, chemistry, and function of microencapsulated pancreatic islets. Biomaterials 24:305–312.

Gibbs BF, Kermasha S, Alli I, Mulligan CN. 1999. Encapsulation in the food industry: A review. Int J Food Sci Nutr 50:213–224.

Grumann M, Brenner T, Beer C, Zengerle R, Ducrée J. 2005. Visualization of flow patterning in high-speed centrifugal microfluidics. Rev Sci Instrum 76:025101.

Haeberle S, Naegele L, Burger R, Zengerle R, Ducrée J. 2007a. Alginate micro-bead fabrication on a centrifugal microfluidics platform. In Proceedings of 19th International Conference on Micro Electro Mechanical Systems (MEMS 2007). Kobe, Japan. pp 497–500.

Haeberle S, Zengerle R, Ducrée J. 2007b. Centrifugal generation and manipulation of droplet emulsions. Microfluidics Nanofluidics 3:65–75.

Joki T, Machluf M, Atala A, Zhu JH, Seyfried NT, Dunn IF, Abe T, Carroll RS, Black PM. 2001. Continuous release of endostatin from microencapsulated engineered cells for tumor therapy. Nat Biotechnol 19:35–39.

Kailasapathy K. 1999. Microencapsulation of probiotic bacteria: Technology and potential applications. Curr Issues Intest Microbiol 3:39–48.

Koch S, Schwinger C, Kressler J, Heinzen C, Rainov NG. 2003. Alginate encapsulation of genetically engineered mammalian cells: Comparison of production devices, methods and microcapsule characteristics. J Microencapsulation 20:303–316.

Lee GM, Gray JJ, Palsson BO. 1991. Effect of trisodium citrate treatment on hybridoma cell viability. Biotechnol Techniques 5:295–298.

Lim F, Sun AM. 1980. Microencapsulated islets as bioartificial endocrine pancreas. Science 210:908–910.

Liu K, Ding HJ, Liu J, Chen Y, Zhao XZ, Liu K, Ding HJ, Liu J, Chen Y, Zhao XZ. 2006. Shape-controlled production of biodegradable calcium alginate gel microparticles using a novel microfluidic device. Langmuir 22:9453–9457.

Martinsen A, Skjakbraek G, Smidsrod O. 1989. Alginate as immobilization material. 1. Correlation between chemical and physical-properties of alginate gel beads. Biotechnol Bioeng 33:79–89.

Orive G, Hernandez RM, Gascon AR, Calafiore R, Chang TM, De VP, Hortelano G, Hunkeler D, Lacik I, Shapiro AM, et al. 2003. Cell encapsulation: promise and progress. Nat Med 9:104–107.

Peirone M, Ross CJD, Hortelano G, Brash JL, Chang PL. 1998. Encapsulation of various recombinant mammalian cell types in different alginate microcapsules. J Biomed Mat Res 42:587–596.

Prusse U, Fox B, Kirchhoff M, Bruske F, Breford J, Vorlop KD. 1998. The Jet Cutting Method as a new immobilization technique. Biotechnol Tech 12:105–108.

Renken A, Hunkeler D. 1998. Microencapsulation: A review of polymers and technologies with a focus on bioartificial organs. Polimery 43:530–539.

Streule W, Lindemann T, Birkle G, Zengerle R, Koltay P. 2004. PipeJet: a simple disposable dispenser for the nano- and microliter range. J Assoc Lab Automation 9:300–306.

Sugiura S, Oda T, Aoyagi Y, Matsuo R, Enomoto T, Matsumoto K, Nakamura T, Satake M, Ochiai A, Ohkohchi N, et al. 2007. Microfabricated airflow nozzle for microencapsulation of living cells into 150 micrometer microcapsules. Biomed Microdev 9:91–99.

Sugiura S, Oda T, Izumida Y, Aoyagi Y, Satake M, Ochiai A, Ohkohchi N, Nakajima M. 2005. Size control of calcium alginate beads containing living cells using micro-nozzle array. Biomaterials 26:3327–3331.

Sultana K, Godward G, Reynolds N, Arumugaswamy R, Peiris P, Kailasapathy K. 2000. Encapsulation of probiotic bacteria with alginate-starch and evaluation of survival in simulated gastro-intestinal conditions and in yoghurt. Int J Food Microbiol 62:47–55.

Tan W-H, Takeuchi S. 2006. Arrayed monodisperse micro-alginate beads in μ-fluidic traps for cell assay. In Proceedings of 19th International Conference on Micro Electro Mechanical Systems (MEMS 2006). Istanbul, Turkey. p 534–537.

Utada AS, Lorenceau E, Link DR, Kaplan PD, Stone HA, Weitz DA. 2005. Monodisperse double emulsions generated from a microcapillary device. Science 308:537–541.

Wolters GHJ, Fritschy WM, Gerrits D, Vanschilfagaarde R. 1992. A versatile alginate droplet generator applicable for micro-encapsulation of pancreatic-islets. J Appl Biomat 3:281–286.